

# KINETICS OF DECOMPOSITION OF DIFFERENT ACID CALCIUM PHOSPHATES

Alexandra Ioițescu, Gabriela Vlase, T. Vlase\* and N. Doca

West University of Timișoara, Research Center for Thermal Analysis in Environmental Problems, Str. Pestalozzi No.16  
Timișoara, 300115, Romania

The kinetics of thermal decomposition of  $\text{Ca}(\text{H}_2\text{PO}_4)_2 \cdot \text{H}_2\text{O}$  under non-isothermal conditions was studied. The TG/DTG curves were obtained at five heating rates: 5, 7, 10, 12 and 20  $\text{K min}^{-1}$ .

The kinetic analysis was performed by means of three methods: Friedman, Budrugač–Segal and NPK by Sempere and Nomen. An important dependence of the activation energy vs. the conversion degree was observed and also a compensation effect. The decomposition consists of water loss and is due to the elimination of crystallization water and an intermolecular condensation, respectively.

**Keywords:** calcium phosphates, non-isothermal kinetics, thermal analysis

## Introduction

Being similar in chemical composition and structure to the biological bone, calcium phosphates have demonstrated excellent biocompatibility and the ability to form a continuous interface with the natural tissue.

The aim of the present paper was to perform a kinetic study on the thermal decomposition of  $\text{Ca}(\text{H}_2\text{PO}_4)_2 \cdot \text{H}_2\text{O}$ , the expected advantage comparing with other precursors for bone-implant materials being the formation of the P–O–P bond due to intermolecular dehydrations. In some previous papers [1–4] the possibilities to characterize different precursors for pharmaceuticals, food additives and biomaterials type products using the thermal analysis and non-isothermal kinetics methods were demonstrated.

The literature presents data on thermal decomposition of calcium phosphate structures, namely: thermal analysis of apatitic structure [5] and kinetic aspects of the thermal decomposition of natural phosphate and its kerogen [6], but nothing about the kinetic of formation of pyro- and polyphosphates by means of thermal treatment of an adequate precursor, so the need to perform a kinetic analysis on phosphatic samples under non-isothermal conditions is understood.

## Experimental

The substance used was monohydrated monocalcium orthophosphate  $\text{Ca}(\text{H}_2\text{PO}_4)_2 \cdot \text{H}_2\text{O}$ , 97.07%, Obrotu Odczynnikami Gliwice.

The thermal decomposition was performed on a Perkin-Elmer TGA7 Thermobalance under nitrogen atmosphere, using a Pt crucible. Five heating rates were used, namely: 5, 7, 10, 12, 20  $\text{K min}^{-1}$ , from ambient temperature to 500°C.

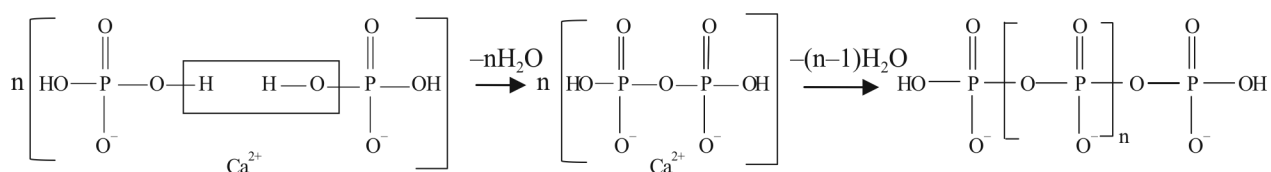
## Results and discussion

The TG and DTG curves are depicted in Fig. 1.

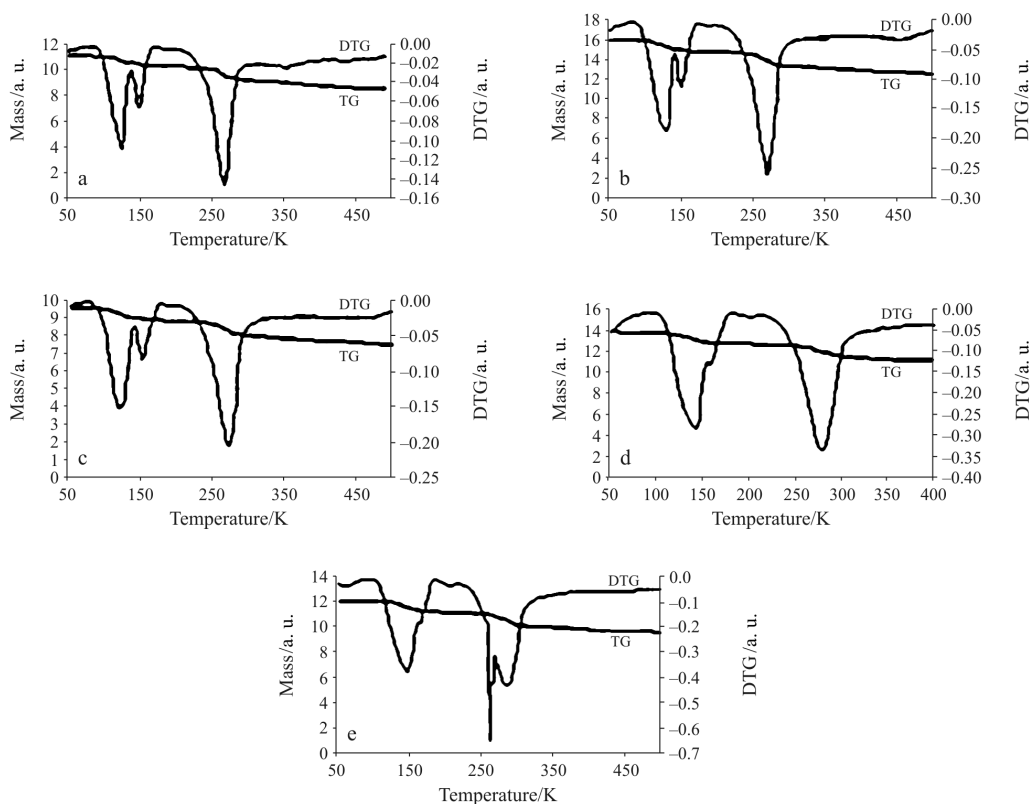
In all cases three processes take place, processes that were called A, B and C. While for a low heating rate the three processes were well defined, for higher heating rates they tend to unify (A and B) or differentiate into two new processes (C).

Table 1 presents, for every heating rate, the temperatures of the beginning ( $T_i$ ) and end ( $T_f$ ) of each process respectively, the temperature of the maximum decomposition rate ( $T_{\text{max}}$ ) and the mass loss  $\Delta m$  (%). Average values of the mass loss were calculated for each process and also a total value of 16.32 was calculated.

A mechanism for this decomposition was suggested, based on the following chemical reaction:



\* Author for correspondence: tvlase@cbg.uvt.ro



**Fig. 1** Curves of monohydrated monocalcium phosphate, heating rates of a – 5, b – 7, c – 10, d – 12, e – 20 K min<sup>-1</sup>

**Table 1** The characteristics of the thermal behavior of Ca(H<sub>2</sub>PO<sub>4</sub>)<sub>2</sub>·H<sub>2</sub>O

Heating rate/ K min <sup>-1</sup>	Process A				Process B				Process C			
	<i>T</i> <sub>i</sub>	<i>T</i> <sub>max</sub>	<i>T</i> <sub>f</sub>	Δ <i>m</i> /%	<i>T</i> <sub>i</sub>	<i>T</i> <sub>max</sub>	<i>T</i> <sub>f</sub>	Δ <i>m</i> /%	<i>T</i> <sub>i</sub>	<i>T</i> <sub>max</sub>	<i>T</i> <sub>f</sub>	Δ <i>m</i> /%
5	90	124	138	5.10	138	148	172	2.04	214	268	304	9.54
7	92	130	142	5.31	141	152	174	1.70	224	270	304	8.80
10	98	122	142	4.99	144	154	178	1.74	226	274	308	8.83
12	102	142	156	5.93	156	160	180	1.08	228	280	318	9.56
20	104	148	162	5.94	162	166	184	1.03	232	262	364	10.03

Based on this mechanism, a formula for the mass loss was obtained [4]:

$$\Delta m = \frac{(2n-1)18}{234n} \cdot 100 \quad (1)$$

where *n* is the number of phosphate ions bound together in the polycondensate chain, and Δ*m* is the mass loss.

Figure 2 is the representation of the water loss (Δ*m*) as a function of *n*, based on Eq. (1).

It is observed that for *n* → ∞, Δ*m* → 15.4%, value which is in good agreement with the practical value obtained for the mass loss, of 16.32%.

It was also noticed that Δ*m* for the processes A and B sums 6.97%, comparing to the value of the theoretical Δ*m* for *n*=1, which is 7.14%. This leads to the

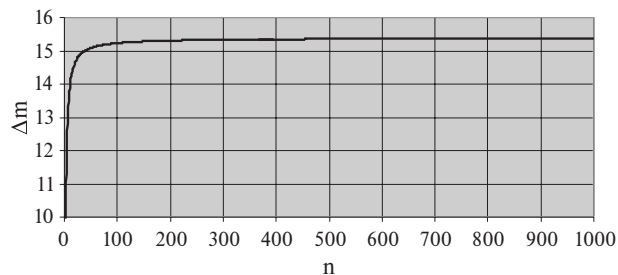


**Fig. 2** Mass loss as a function of the polycondensation degree (Eq. (1))

conclusion that processes A and B represent the loss of the crystallization water, which happens quicker for higher heating rates.

It was so concluded that an initial crystallization water loss process (A and B steps in the curves) takes place, followed by intermolecular dehydrations (polycondensations).

### Kinetic analysis

Based on the three decomposition steps observed, a kinetic study was performed.

First the differential isoconversional method of Friedman was used [7], based on equation:

$$\beta \frac{d\alpha}{dT} = f(\alpha) A \exp\left(-\frac{E}{RT}\right) \quad (2)$$

or the equivalent:

$$\ln\left(\beta \frac{d\alpha}{dT}\right) = \ln[Af(\alpha)] - \frac{E}{RT} \quad (3)$$

where  $\alpha$  – the conversion degree,  $\beta$  – the heating rate,  $A$  – the preexponential factor,  $E$  – activation energy.

For a constant conversion, the slope and the intercept of the graphical representation of  $d\alpha/dt$  vs.  $1/T$  give the activation energy value ( $E$ ), and the  $Af(\alpha)$  value respectively.

The values of the activation energy with Friedman method are presented in Table 2.

For all the three processes a significant variation of the activation energy vs. the conversion degree was observed.

This is a sign of the existence of more than one process in the case of the dehydration – polyconden-

sation reaction. Therefore more sophisticated data processing should be used.

The first suggested is the method of Budrugaec and Segal [8, 9] which takes into account a dependence of  $E$  vs.  $\alpha$  in the form of:

$$E = E_0 + E_1 \ln(1-\alpha) \quad (4)$$

where  $E_0$  and  $E_1$  are constants. Indeed, the data in Table 2 are in good agreement with Eq. (4), as presented in Fig. 3.

Another important hypothesis of the B–S method is the existence of a compensation effect, i.e.:

$$\ln A = aE + b \quad (5)$$

In Fig. 4 the existence of the compensation effect is proved for all the three dehydration steps, using the data of Friedman processing:

With Eqs (4) and (5), considering a conversion function

$$f(\alpha) = (1-\alpha)^n \quad (6)$$

the Eq. (3) became:

$$\ln\left(\beta \frac{d\alpha}{dT}\right) = \left(b + aE_0 - \frac{E_0}{RT}\right) + \left(aE_1 - \frac{E_1}{RT} + n\right) \ln(1-\alpha) \quad (7)$$

The correct value of  $n$  will be the one that gives the correlation coefficient closest to 1.

The values obtained by processing with the B–S method are systematized in Table 3.

The values of  $E_0$  for both A and B steps are very near, an argument for considering these steps to correspond to the same process, i.e. the loss of the crystalli-

**Table 2** Activation energy with Friedman's method

Conversion %	0.1	0.2	0.3	0.4	0.5	0.6	0.7	0.8	0.9
$E_A/J \text{ mol}^{-1}$	153.8 ±0.52	136.2 ±0.44	121.4 ±0.57	101.8 ±0.35	82.6 ±0.25	73.7 ±0.21	64.4 ±0.17	52.7 ±0.09	26.4 ±0.03
$E_B/J \text{ mol}^{-1}$	141.4 ±0.068	132.3 ±0.061	119.3 ±0.047	109.8 ±0.048	103.1 ±0.069	97.3 ±0.082	96.4 ±0.1	108.7 ±0.14	74.4 ±0.11
$E_C/J \text{ mol}^{-1}$	145.8 ±0.53	165.8 ±0.51	165 ±0.42	142.9 ±0.44	124 ±0.37	104.9 ±0.33	81.9 ±0.34		

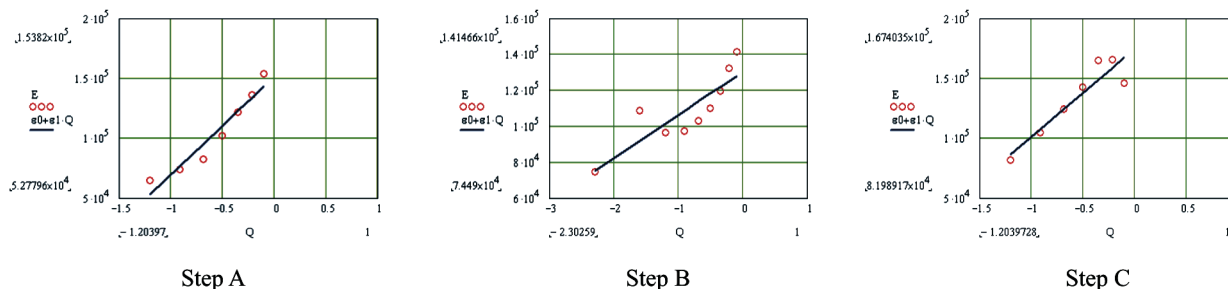


**Fig. 3** The dependence of the activation energy vs.  $\ln(1-\alpha)$

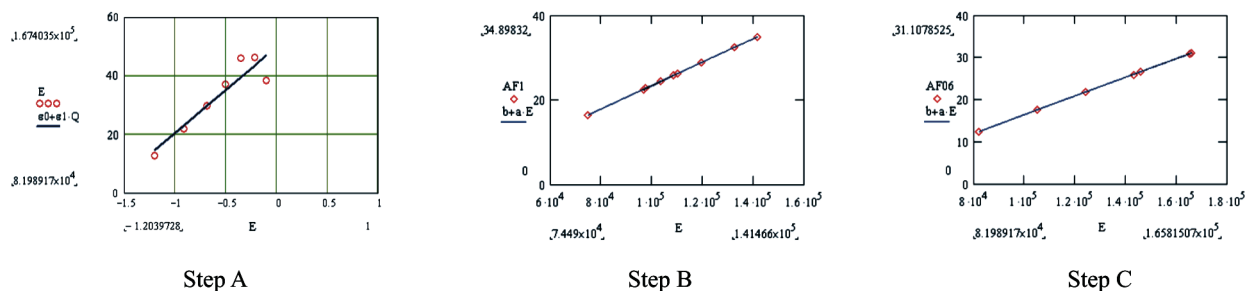


Fig. 4 Diagrammatic description of the compensation effect as  $\ln(Af(\alpha))$  vs.  $E$

Table 3 Budrugeac–Segal parameters

Process	$E_0/\text{J mol}^{-1}\cdot 10^{-8}$	$E_1/\text{J mol}^{-1}\cdot 10^{-7}$	$a\cdot 10^4/\text{mol J}^{-1}$	$b$	Correlation coefficient	$n$
A	1.5215±0.1542	8.2532±1.0169	3.1100±0.0139	-6.8921±0.3412	0.99995	0.1
B	1.3031±0.090	2.39532±0.5961	2.76571±0.0033	-4.2269±0.0815	1	1.0
C	1.75168±0.20376	7.36959±1.3438	2.225564±0.0068	-5.8413±0.1929	0.999979	0.6

zation water. A smaller  $E_1$  value for B step in comparison with A explains the tendency to unify at higher heating rates (a higher thermal ‘sensitivity’ of step B).

Taking into account some previous results on kinetic analysis of thermal decomposition of alkaline phosphates [10], the study was continued with the non-parametric kinetic [11–13] method.

The experimental data are represented in a 3D space ( $d\alpha/dt$ ,  $T$ ,  $\alpha$ ) and interpolated to generate a continuous surface of the reaction rate:

$$\frac{d\alpha}{dt} = f(T)g(\alpha) \quad (8)$$

Such a surface is depicted in Fig. 5.

This surface is discretized as a square  $i \times j$  matrix  $M$ , where the rows correspond to different degrees of conversion  $\alpha_1-\alpha_i$  and the columns to different temperatures  $T_1-T_j$ .

The NPK method uses the single value decomposition (SVD) algorithm [14] to decompose matrix  $M$ .

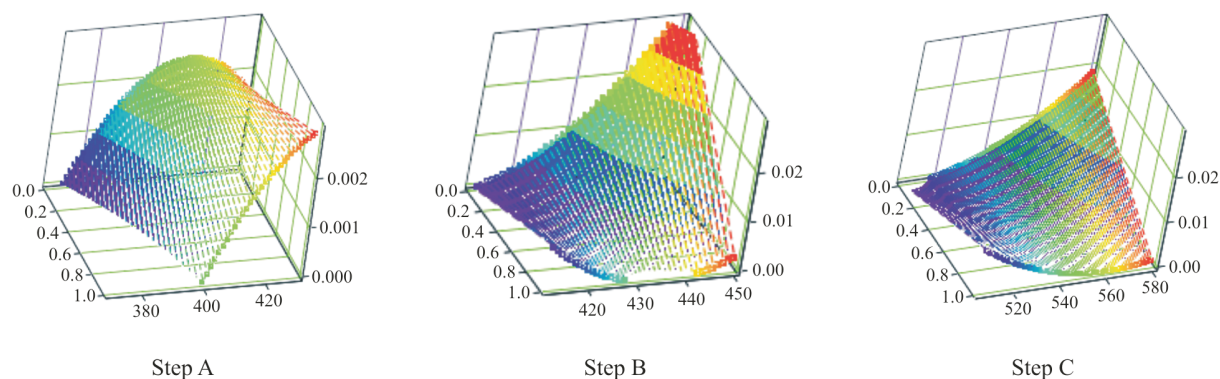


Fig. 5 The reaction rate surface in a 3D space

Table 4 Kinetic parameters with NPK method

Reaction step	Explained variance of the process/ $\lambda\%$	$E/\text{kJ mol}^{-1}$	$A/\text{min}^{-1}$	$M$	$n$	Corr.
A	82.8	36.6±8.6	$1.3\cdot 10^4 \pm 1.3\cdot 10^3$	1	1	0.9760
	15.6	53.6±6.3	$3.1\cdot 10^6$	0	1/4	0.9960
B	95	104.0±1.5	$6.8\cdot 10^{11} \pm 3.12$	0	1	0.9999
	5	589.0±76.9	$2.2\cdot 10^{68}$	0	1	0.9999
C	80	84.2±6.6	$2.6\cdot 10^7 \pm 61$	0	3/2	0.9996
	19	52.3±12.4	$7.0\cdot 10^4$	3/2	3/2	0.9997

$$M=U(\text{diag}.D)V^T \quad (9)$$

The vector  $u_1$ , given by the first column of the matrix  $U$ , is analysed *vs.*  $\alpha$  to determine the kinetic model, whereas  $v_1$ , the first column of matrix  $V$ , is analysed *vs.*  $T$ .

For temperature dependence, the Arrhenius equation was checked, and for the kinetic model the Šesták–Berggren equation [15] was suggested:

$$g(\alpha)=\alpha^m(1-\alpha)^n \quad (10)$$

The singular value vector  $s$  takes into account the number of steps of the reaction. If

$$M=M_1+M_2 \quad (11)$$

it means that the reaction step has two elementary processes and the discrimination between them depends on the values of the corresponding explained variance  $\lambda_1$  and  $\lambda_2$  ( $\lambda_1+\lambda_2=100$ ).

The data of the NPK analysis are systematized in Table 4.

The kinetics of step A is described by a preponderant and a secondary process. This preponderant process is a first order chemical process ( $n=1$ ), accompanied by diffusion ( $m=1$ ). The secondary process can not be totally neglected as the  $E$  value is not quite different from that of the preponderant process.

In case of step B, there is practically a single step. The value is too high in comparison with step A and this is again an explanation of the tendency to unify steps A and B at higher heating rates.

Step C exhibits a higher activation energy in comparison with step A, and this is understandable because step C corresponds to a true P–OH bond breaking, in connection with the polycondensation reaction. Also the appearance of a physical factor in the secondary process can be ascribed to the diffusional limitations by water elimination at high polycondensation degrees.

## Conclusions

- By thermal treatment of  $\text{Ca}(\text{H}_2\text{PO}_4)_2 \cdot \text{H}_2\text{O}$  under non-isothermal conditions, three mass loss steps were evidenced. These correspond to the loss of crystallization water (the first two), respectively to

a continuous intermolecular polycondensation and elimination of water.

- For a deeper understanding of these steps a carefully kinetic analysis is necessary. This analysis reveals an important dependence of the activation energy on the degree of conversion and also the existence of a compensation effect.
- From the three utilized methods for kinetic analysis, the NPK is able to offer kinetic parameters and details on the reaction mechanism in a less speculative manner. A diffusional limitation (due to the water elimination) towards the last part of the polycondensation was observed.

## References

- 1 T. Vlase, G. Vlase and N. Doca, *J. Therm. Anal. Cal.*, 80 (2005) 207.
- 2 T. Vlase, G. Vlase, M. Doca and N. Doca, *J. Therm. Anal. Cal.*, 72 (2003) 597.
- 3 T. Vlase, G. Jurca and N. Doca, *J. Therm. Anal. Cal.*, 67 (2002) 597.
- 4 A. Popovici, A. Ioitescu and N. Doca, *Annals of West University of Timișoara, Series of Chemistry*, 15 (2006) 83.
- 5 K. Tönsuaadu, M. Peld and V. Bender, *J. Therm. Anal. Cal.*, 72 (2003) 363.
- 6 A. Aouad, L. Bilali, M. Benchanâa and A. Mokhlisse, *J. Therm. Anal. Cal.*, 67 (2002) 733.
- 7 H. L. Friedman, *J. Polymer Sci.*, 6C (1965) 183.
- 8 P. Budrugaec and E. Segal, *J. Therm. Anal. Cal.*, 62 (2001) 821.
- 9 P. Budrugaec and E. Segal, *J. Therm. Anal. Cal.*, 66 (2001) 557.
- 10 T. Vlase, G. Vlase, A. Chiriac and N. Doca, *J. Therm. Anal. Cal.*, 80 (2005) 87.
- 11 R. Serra, R. Nomen and J. Sempere, *J. Therm. Anal. Cal.*, 52 (1998) 933.
- 12 R. Serra, J. Sempere and R. Nomen, *Thermochim. Acta*, 316 (1998) 37.
- 13 J. Sempere, R. Nomen and R. Serra, *J. Therm. Anal. Cal.*, 56 (1999) 843.
- 14 M. E. Wall, 'Singular value decomposition and principal component analysis' in 'A practical approach to microarray data analysis, 9. 91-109, Kluwer, Norvel MA (2003).
- 15 J. Šesták and G. Berggren, *Thermochim. Acta*, 3 (1971) 1.

DOI: 10.1007/s10973-006-8022-3